Keggin-type polyoxometalates as Cu(ii) chelators in the context of Alzheimer's disease

Elena Atrián-Blasco, Lucie de Cremoux, Xudong Lin, Rufus Mitchell-Heggs, Laurent Sabater, Sébastien Blanchard, Christelle Hureau

Keggin-type Polyoxometalates as Cu(II) chelators in the context of Alzheimer's disease.

Elena Atrián-Blasco,[a,b,#] Lucie de Cremoux,[a,#] Xudong Lin,[a] Rufus Mitchell-Heggs,[a] Laurent Sabater,[a] Sébastien Blanchard[c,*] and Christelle Hureau[a,*]

Two Keggin polyoxometalates were used as new copper ligands to counteract the effects of Cu^{II}(Amyloid-β) interaction. Their ability to remove Cu^{II} from Cu^{II}(Amyloid-β), to stop Cu^{II}(Amyloid-β) induced formation of reactive oxygen species and to restore apo-like self-assembly of Cu^{II}(Amyloid-β) were shown.

Alzheimer's disease (AD) is a debilitating and devastating mental disorder and the most widespread kind of dementia. Due to the aging of the population and the lack of curative treatments, the number of AD patients will increase dramatically in the near future, putting the health care system under an incredibly huge pressure.[1] This underlines the need for alternatives to the current therapeutic options. AD is characterized by the presence of extra-cellular deposits of highly ordered supra-molecular assemblies of the Amyloid-β (Aβ) peptide, the so-called senile or amyloid plaques in specific regions of the brain. The Aβ peptide indeed belongs to the amyloid-forming peptides family that also include amylin and α-synuclein, involved in Type II diabetes and Parkinson's diseases respectively.[2] The main forms of Aβ peptides are made of 39 to 43 amino acids residues, with the 40 amino-acids sequence being the most studied. In addition to a N-terminal hydrophilic part (up to the 16 residues), the peptide is made of a central hydrophobic core encompassing residues LVVF and of a C-terminal hydrophobic part, both involved in the self-assembly ability of the peptide. This process known as aggregation finally leads to the formation of highly stable β-sheets rich supramolecular structures (amyloids) that gather into the senile plaques.[3] The 16 residues N-terminal sequence contains several metal binding residues (mainly histidine and carboxylate-containing residues) involved in the coordination of d-block ions, mainly Copper and Zinc.[2] Based on that ability and the abnormally high level of Cu, Zn and Fe found in the senile plaques, and in line with many *in vitro* studies that have shown a role of metal ions in the modulation of Aβ self-assembly, metal ions are regarded as biologically relevant partner of amyloid formation and related toxicity.[2, 4, 5] In addition to the Aβ aggregation, oxidative stress is the other key event in the etiology of AD. Cu-bound to Aβ can catalyze the production of Reactive Oxygen Species (ROS) and thus may contribute to the overall oxidative stress observed in the disease.[6]

Polyoxometalates are oxoclusters of early transition metal ions that have found applications in various fields from catalysis to material science. They result from the polycondensation in acidic media of oxoanions such as WO_4^{2-}, templated or not by p-oxoanions (PO_4^{3-}, SiO_4^{4-}, etc.). Furthermore, controlled basic degradation of complete POMs can lead to lacunary POMs, which are very efficient all-inorganic ligands. Among the vastly proposed biochemical and medical applications of polyoxometalates,[7-9] their interactions with peptides and proteins have been gaining interest over the last years.[10, 11] For example, Prusiner and co-workers have studied the ability of different POMs, mainly Keggin-type (Scheme 1), to promote the aggregation of the toxic form of the prion protein.[12] The modulating activity of these polyoxoanions relies on their electrostatic interactions with the positively charged amino acids of the protein, while the size of the POM may also play a role.[13] While it has been proposed that various types of POMs could modulate Aβ aggregation via electrostatic interaction,[14-16] Qu et al. reported that transition metal substituted POMs (MS-POMs) were even more efficient, presumably via additional coordination bond between metal ion and the histidine residues of Aβ.[17] While POMs, including MS-POM, were used to tune Aβ self-assembly, there is no report on the use of POMs as chelating agents (in the context of AD), although giant POMs were shown to alter Cu(II)Aβ and Zn(II)Aβ aggregation due to multiple weak electrostatic interactions with metal ions.[16] Up to now, no lacunary POM has been studied for its ability to host

[a] *LCC-CNRS, Université de Toulouse, CNRS, Toulouse, France*
[b] *Instituto de Nanociencia y Materiales de Aragón (INMA), Consejo Superior de Investigaciones Científicas-Universidad de Zaragoza, 50009 Zaragoza, Spain*
[c] *CNRS, Institut Parisien de Chimie Moléculaire, IPCM, Sorbonne Université, 4 Place Jussieu, F-75005 Paris, France , # contribute equally to the work.*
†Electronic Supplementary Information (ESI) available: [details of any supplementary information available should be included here]. See DOI: 10.1039/x0xx00000x

a dication to remove Cu^{II} bound to Aβ and to prevent resulting effects with respect to Aβ aggregation and Cu(Aβ)-induced ROS production and thus to act as a classical chelator but with the extra ability to modify Aβ aggregation on its own. This is the core of the present communication, where we present a detailed study of the influence of $K_4[\alpha\text{-}SiW_{12}O_{40}]$ ($K_4\alpha[\mathbf{K}]\cdot 10H_2O$) and its monolacunary derivative $K_8[\alpha\text{-}SiW_{11}O_{39}]$ ($K_8\alpha[\mathbf{K_\ell}]\cdot 18H_2O$) on Cu and Cu(Aβ)-induced ROS production and on aggregation of Aβ (with or without Cu^{II} being present). This first study may open new routes of research with POM as efficient chelating agent in the AD context.

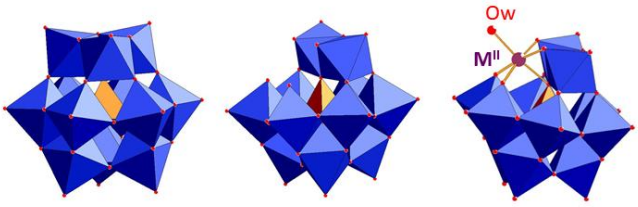

Scheme 1. $\mathbf{K^{4-}}$, $\mathbf{K_\ell^{8-}}$ and $\mathbf{K_M^{6-}}$ structures (M^{II} is a d-metal dication, w = water molecule).

$\mathbf{K^{4-}}$ and $\mathbf{K_\ell^{8-}}$ structures (Scheme 1) are composed of a central Si(IV) surrounded by four atoms of oxygen, which connect the central Si to twelve ($\mathbf{K^{4-}}$) or eleven ($\mathbf{K_\ell^{8-}}$) W(IV) cations each in an octahedral WO_6 environment. Since $\mathbf{K^{4-}}$ is known to generate $\mathbf{K_\ell^{8-}}$ at pH > 4,[18] (and ref. therein) we probed this transformation under our working conditions. Evolution of the O to W charge transfer bands around 240 nm in a pH 6.9 HEPES buffer shows that this conversion takes place over 90 minutes (Fig. S1, A) while $\mathbf{K_\ell^{8-}}$ is stable (Fig. S1, B) in line with reported aqueous solution stability properties.[19] In the presence of Cu(II), the formation of the $[\alpha\text{-}SiW_{11}O_{39}Cu(OH_2)]^{6-}$ ($\mathbf{K_{Cu}^{6-}}$) anion from $\mathbf{K^{4-}}$ or $\mathbf{K_\ell^{8-}}$, respectively takes about one hour or is instantaneous as attested by the kinetic monitoring of the appearance of a new band at 253 nm corresponding to the generation of a MS-POM (Fig. S1, panels C and D). Coordination of Cu(II) to the POM anion is also confirmed by a broad and very weak d-d band with maximum at 865 nm (ε = 40 $M^{-1}cm^{-1}$) and an EPR spectrum characteristic of a Cu(II) ion lying in a D4h geometry surrounded by five oxygen atoms from the POM skeleton and a water molecule (Figure1, A, and C), in line with literature.[20]

Once the ability of $\mathbf{K^{4-}}$ and $\mathbf{K_\ell^{8-}}$ to coordinate Cu(II) was checked, their ability to retrieve Cu(II) bound to Aβ was studied. The evolution of the characteristic d-d band of the Cu(Aβ) complex at 625 nm was followed by UV-vis spectroscopy after the addition of either $\mathbf{K_\ell^{8-}}$ or $\mathbf{K^{4-}}$ (Figure 1, panel A and B). The observed full disappearance of the Cu(Aβ) signature indicates that both POMs can completely remove Cu(II) from the peptide to form the $\mathbf{K_{Cu}^{6-}}$. While the removal has a time of half completion of 40 minutes with $\mathbf{K^{4-}}$, it is instantaneous with $\mathbf{K_\ell^{8-}}$. This was also observed by EPR, where $\mathbf{K^{4-}}$ completely removes Cu(II) from Aβ after a 3-hours incubation time while the EPR spectrum measured just after addition of $\mathbf{K_\ell^{8-}}$ to a Cu(Aβ) solution shows already signatures of the $\mathbf{K_{Cu}^{6-}}$ as a largely predominant species (Figure 1, panel C).

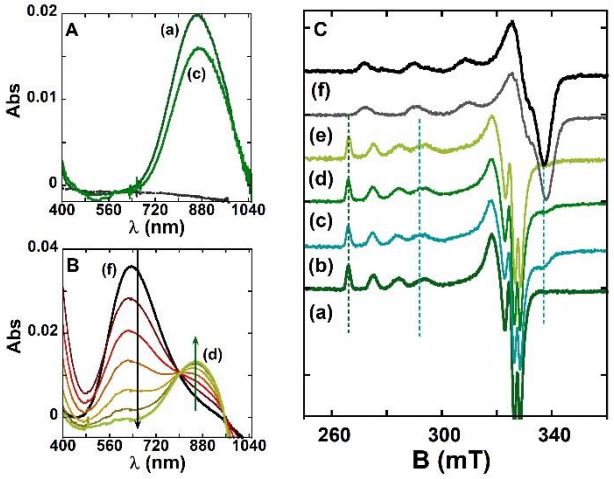

Figure 1. (**A**) UV-Vis spectra in the d-d region of Cu(II) + $\mathbf{K_\ell^{8-}}$ (a, dark green) and Cu(Aβ) + $\mathbf{K_\ell^{8-}}$ -(c, green), (**B**) Kinetic monitoring of Cu(Aβ) + $\mathbf{K^{4-}}$; (f, black) starting spectrum and (d, green) last spectrum, once the reaction is completed. Spectrum measured at 5 (brown), 20 (red), 40 (dark orange), 70 (light brown), 110 (dark brown) and 170 minutes (light green, d) after the addition of $\mathbf{K^{4-}}$ to Cu(Aβ). Conditions: $[A\beta_{16}] = [\mathbf{K^{4-}}] = 500\ \mu M$, [Cu(II)] = 450 μM, [HEPES] = 100 mM pH 6.9, ℓ = 1 cm, the solution was continuously stirred and the temperature controlled at 25 °C. (**C**) EPR spectra of: Cu(Aβ) (f, black); Cu(Aβ) + $\mathbf{K^{4-}}$ at t_0 (e, grey) and t_f (d, light green); Cu(Aβ) + $\mathbf{K_\ell^{8-}}$ (c, green, at t_0 or t_f), Cu(II) + 4 equiv. (Aβ) + 1 equiv. $\mathbf{K_\ell^{8-}}$ (b, turquoise) and Cu(II) + $\mathbf{K_\ell^{8-}}$ (a, dark green). Spectra at t_0 were taken just after the addition of $\mathbf{K_\ell^{8-}}$ or $\mathbf{K^{4-}}$ to the Cu(Aβ) solution, and after 1 day of incubation for t_f. Conditions: $[A\beta_{16}] = [\mathbf{K_\ell^{8-}}$ or $\mathbf{K^{4-}}] = 200\ \mu M$, $[^{65}Cu(II)] = 180\ \mu M$, [HEPES] = 100 mM pH 6.9, 10% glycerol added as cryoprotectant. ν = 9.47 GHz, T = 120 K, microwave power = 20 mW, Modulation Amplitude = 0.5 mT.

The thorough inspection of the UV-Vis but mainly the EPR spectrum of the complex formed by the addition of $\mathbf{K^{4-}}$ or $\mathbf{K_\ell^{8-}}$ to Cu(Aβ) slightly differs from that of the *in situ* generated $\mathbf{K_{Cu}^{6-}}$ (without Aβ). An additional small peak at 335 mT is indeed detected (Figure 1, panel C, blue vertical line). Linear combinations of the EPR spectra of Cu-Aβ and $\mathbf{K_{Cu}^{6-}}$, which could mirror the incomplete removal of Cu(II) from Aβ by the POMs, failed to reproduce this EPR signal thus pointing strongly toward the formation of a ternary species. While deciphering its exact nature is beyond the scope of the present communication, we propose that this species corresponds to a complex between $\mathbf{K_{Cu}^{6-}}$ and Aβ, where Aβ may bind the Cu(II) ion on its sixth labile position. This is confirmed by the increase of the relative intensity of the peak induced by the presence of higher ratio of Aβ versus $\mathbf{K_{Cu}^{6-}}$ (Figure 1, panel C). This proposition is in line with the lability of the water molecule bound to the MS-POMs,[21] and with reported interaction of Cu(II) in MS-POM with the imidazole from histidine side-chains of Aβ peptides.[17]

Since $\mathbf{K^{4-}}$ and $\mathbf{K_\ell^{8-}}$ can bind Cu(II) out from the Aβ peptide (although with different rates), their ability to stop the Cu(Aβ)-induced ROS production was assayed. This was done with a well-established ascorbate (Asc) consumption experiment that mirrors the production of ROS.[22] Briefly, under aerobic conditions, Asc fuels the incomplete reduction of dioxygen and thus the formation of ROS. The Asc consumption is catalysed by the presence of Cu^{II} or Cu^{II}(Aβ) leading to the decrease of the absorbance at 265 nm (corresponding to ascorbate, ε = 14500 $M^{-1}cm^{-1}$). Two experiments were performed, either starting from the +II redox state and including a short incubation with

the POM (c.a. 60 s) or with the POM added in the course of Asc consumption (when absorbance equals 1), thus in presence of both Cu^{I} and Cu^{II} ions. K_{ℓ}^{8-} can prevent the Asc consumption, both starting from Cu^{II} and $Cu^{II}(A\beta)$ or when added in the course of the experiment. There is indeed no decrease in the Asc UV band in presence of K_{ℓ}^{8-} (Figure 2, panel A). In contrast, K^{4-} is active only if incubated before Asc addition (Figure 2, panel B), in line with the longer time required to form the K_{Cu}^{6-} species.

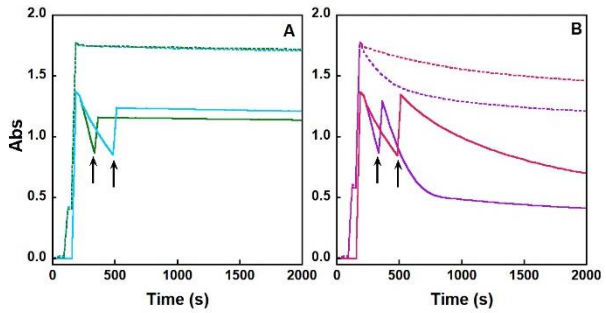

Figure 2. Absorption (measured at 265 nm) monitoring of the effect K_{ℓ}^{8-} (panel A) and K^{4-} (panel B) on Cu^{II} and $Cu^{II}(A\beta)$-induced Asc consumption. (**A**) dotted lines: data with Cu^{II} (green) and $Cu^{II}(A\beta)$ (blue) incubated first with K_{ℓ}^{8-} during 60 s; plain lines: data with K_{ℓ}^{8-} added when Abs is at ca. 1 (indicated by arrows), during Asc consumption catalysed by Cu^{II} (green) and $Cu^{II}(A\beta)$ (blue). Before POM addition the curves corresponds to Asc consumption by Cu^{II} and $Cu^{II}(A\beta)$. (**B**) dotted lines: data with Cu^{II} (purple) and $Cu^{II}(A\beta)$ (pink) incubated first with K^{4-} during 60 s; plain lines: data with K^{4-} added when Abs is at ca. 1, during Asc consumption catalysed by Cu^{II} (purple) and $Cu^{II}(A\beta)$ (pink). $[A\beta_{16}] = [K_{\ell}^{8-}, K^{4-}] = 10\ \mu M$, $[Cu(II)] = 9\ \mu M$, [HEPES] = 100 mM pH 6.9, $\ell = 1$ cm, T = 25 °C.

In addition to its participation to oxidative stress, Cu(II) also affects the aggregation path of the Aβ peptide.[23] This will be under focus in the coming section. The self-assembly of Aβ is a very complex and multi-step mechanism, which can be viewed as a nucleation-elongation supramolecular polymerisation process, in which secondary nucleation by formed amyloids takes a predominant part.[24, 25] The low molecular weight intermediates present during the aggregation are currently regarded as the most toxic species (compared to the starting monomer and the final fibrils) and Cu^{II} has been proposed to promote their formation.[26] To monitor Aβ aggregation, the thioflavin-T (ThT) fluorescence screening assay was used,[27] and the morphology of the aggregates formed was observed after 6 days using Transmission Electronic Microscopy (TEM). Note that as recently pointed out, due to the intrinsic auto-catalytic nature of the aggregation process, the reproducibility of aggregation experiments is fairly weak.[28] To secure robust results, we have thus repeated several times the aggregation assays and have changed several environmental parameters, mainly to avoid the so-called "batch-dependent" results. The results are described based on the data shown in Figure 3 that are representative of the trends observed in all the experiments, and the range of values of the key kinetic parameters of the 3 mathematically-analysed experiments are given in Table S1 (see also Figure S2 for an illustration of the fitting). The aggregation curves for the apo-Aβ peptide‡ show the expected sigmoidal shape (Figure 3, black line) characteristic of amyloids formation,[25, 28] with the time evolution of the fluorescence intensity being described by $F(t) = \frac{\Delta F}{\left(1+e^{-k(t-t_{1/2})}\right)}$ (Eq. 1) .

$t_{1/2}$ is the time necessary to reach half of ΔF, the variation of ThT fluorescence intensity; k is the growth rate mirroring the formation of fibrils. Overall, in presence of K_{ℓ}^{8-} or K^{4-}, the maximum of fluorescence intensity is increased by about 2 to 3-fold and the $t_{1/2}$ is increased by about 10 to 20% compared to Aβ (Figure 3, panel A). The important increase in the final fluorescence reflects the formation of more fibrils and/or the formation of more ordered fibrils inducing a higher enhancement of the ThT fluorescence. No statistically-meaningful differences were observed between K_{ℓ}^{8-} or K^{4-} in line with the quite rapid evolution of K^{4-} to K_{ℓ}^{8-} compared to the time scale of the aggregation (Table S1). By TEM (Figure S3), the pictures show long and twisted Aβ fibrils in absence of POM; while in presence of POM, more abundant and longer fibrils are observed. In presence of Cu^{II}, the aggregation curve shows a two-step aggregation path where the ThT fluorescence increases during the first five hours followed by a second ill-defined and smooth sigmoid-like increase. The resulting fluorescence is weaker than in absence of Cu^{II} by about 15%. This kinetic profile is reminiscent of published data on Cu^{II} modulation of Aβ aggregation,[23] and mirrors the formation of less-ordered aggregates. In presence of K_{ℓ}^{8-} or K^{4-}, the kinetic of the ThT fluorescence is dramatically changed with curves that resemble those obtained upon addition of K_{ℓ}^{8-} or K^{4-} on the apo Aβ (Figure 3, panel B). In the TEM pictures, in presence of Cu^{II}, the Aβ fibrils are shorter, thicker and less abundant than with the apo-peptide, but in presence of POM very long and thin fibrils are recovered. This indicates that the *in-situ* generated K_{Cu}^{6-} has a similar effect on Aβ aggregation than its apo counterparts, K_{ℓ}^{8-} or K^{4-}, id est redirecting the Aβ aggregation towards more fibrillar species. Deeper inspection of the ThT fluorescence curves reveals that the $t_{1/2}$ value of the Cu(Aβ) aggregation in presence of K_{ℓ}^{8-} or K^{4-} is increased by about 20% (Table S1) compared to those of Aβ in presence of K_{ℓ}^{8-} or K^{4-}. Hence, the in situ generated K_{Cu}^{6-} has a slightly increased ability to delay Aβ self-assembly effect compared K_{ℓ}^{8-} (or K^{4-}). This may be linked to the difference in the net charge and in the possibility to form coordination bond between K_{Cu}^{6-} (but not K_{ℓ}^{8-} nor K^{4-}) and some of the amino-acid side chains of the Aβ peptide. Under our working conditions, K_{ℓ}^{8-} / K^{4-} and K_{Cu}^{6-} interact with Aβ promoting the formation of highly ordered fibrils. This is different to previous data on other POM and MS-POM, which were shown to reduce ThT intensity by 40 to 80 % depending on the substituted cations.[15, 17] The origin of such discrepancy has to be understood but will require an in-depth investigation of the modes of interaction of POM with Aβ peptide (currently under investigation) that is beyond the scope of the present communication, while the exact nature of the POM and different working conditions may be part of the explanation. The enhancement of amyloid formation is however highly reminiscent to what has been observed for linear polyphosphates, a biological polyanion.[29] The most remarkable effect of the studied POMs on Cu^{II} modulated Aβ aggregation is their double mode of action. Indeed they (i) remove Cu^{II} from Aβ preventing the formation of ill-defined Cu(Aβ) aggregates, regarded as the most deleterious with respect to AD,[30] and (ii) then the *in situ* generated K_{Cu}^{6-} reshapes

the aggregation kinetic and species towards a better defined sigmoidal process and the formation of mature fibrils, respectively. Most of the ligands reported in the literature can restore apo-aggregation if they are able to retrieve Cu^{II} from Aβ,[31] but have no additional effect.

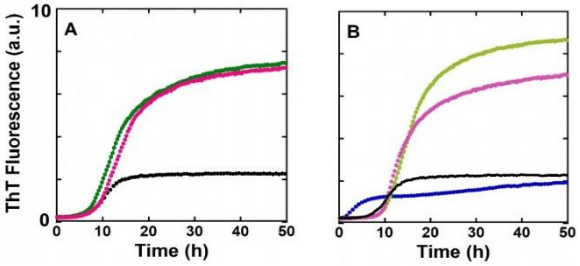

Figure 3. Selection of representative ThT curves of the $A\beta_{1\text{-}40}$ peptide (**A**) or the $Cu(A\beta_{40})$ complex (**B**) in absence or presence of POMs. Panel A: apo-$A\beta_{40}$ (black), $A\beta_{40}$ + 1 equiv. $\mathbf{K^{4-}}$ (pink), $A\beta_{40}$ + 1 equiv. $\mathbf{K_{\varepsilon}^{8-}}$(green). Panel B: $Cu(A\beta_{40})$ (blue) formed at 0.9 equiv. of Cu(II), $Cu(A\beta_{40})$ + 1 equiv. $\mathbf{K^{4-}}$ (light green), $Cu(A\beta_{40})$ + 1 equiv. $\mathbf{K_{\varepsilon}^{8-}}$ (light pink) and apo-$A\beta_{40}$ (black) for direct comparison. Conditions: $[A\beta_{40}]$ = 20 µM, [$\mathbf{K_{\varepsilon}^{8-}}$ or $\mathbf{K^{4-}}$] = 0 or 20 µM, [Cu(II)] = 0 or 18 µM, [ThT] = 10 µM, [EDTA] = 0.1 µM, [HEPES] = 50 mM, pH 6.9, T = 37 °C. The pH was controlled after the completion of the aggregation process and verified to be kept at 6.9 for all conditions. All the curves corresponding to this experiment (noted N°1, are given in the Supporting Information along with simulated curves).

In summary, our results provide new insights on the use of POMs in the context of AD. Their ability to coordinate Cu^{II} out of the Aβ was first assessed: $\mathbf{K_{\varepsilon}^{8-}}$ is readily effective, while $\mathbf{K^{4-}}$ needs first to lose one WO^{4+} unit to form $\mathbf{K_{\varepsilon}^{8-}}$. Once the $\mathbf{K_{Cu}^{6-}}$ has formed a redox inert and stable complex is obtained. Both POM induce the formation of more-ordered Aβ aggregates (higher β-sheet contents) including in the presence of Cu^{II}. Hence the two POM studied here fulfil criteria to be appropriate Cu^{II} chelators in the context of AD. Indeed preventing Cu^{II} interaction with Aβ is of interest for metal-based therapy against AD, as this prevents the formation of toxic oligomers and the deleterious production of ROS. In fact, the POM studied "kill two birds with one stone" since they not only stop Cu(Aβ) ROS production but also redirect aggregation towards mature fibrils regardless the presence of Cu. Previous studies have shown that POMs do not produce toxicity and are capable of passing the blood-brain barrier.[17] Therefore, $\mathbf{K^{4-}}$ and $\mathbf{K_{\varepsilon}^{8-}}$ studied here could be promising drug candidates. In addition, modulation of charge of the POM by playing with the central heteroatom and/or its shape can offer a huge diversity of optimization options. These variations and their effects both on prevention of Cu^{II}- and Cu^{II}(Aβ)-induced ROS and on the modulation of Aβ assembly are currently under study.

Dr. V. Borghesani is acknowledged for her participation in recording preliminary data. E.A.B., L. de C, L.S. and C.H. thank the ERC StG grant 638712, aLzINK for financial support.

Notes and references

‡ The shorter $A\beta_{16}$ peptide has been used as a valuable model for Cu(II) binding to the full length $A\beta_{40}$ or $A\beta_{42}$ peptides for the experiments studying the coordination and the ROS production. The longer $A\beta_{40}$ peptide has been used for the experiments involving aggregation. No differences between the short and full-length Aβ peptides have been observed for their binding Cu(II) coordination, binding affinity or ROS production.[5]

1 Alzheimer's Association, Facts and Figures, https://www.alz.org/alzheimers-dementia/facts-figures).
2 E. Atrian-Blasco, P. Gonzalez, A. Santoro, B. Alies, P. Faller and C. Hureau, *Coord. Chem. Rev.*, 2018, **375**, 38.
3 Z. L. Almeida and R. M. M. Brito, *Molecules*, 2020, **25**.
4 T. J. Huat, J. Camats-Perna, E. A. Newcombe, N. Valmas, M. Kitazawa and R. Medeiros, *J. Mol. Biol.*, 2019, **431**, 1843.
5 C. Hureau in *Alzheimer's Disease: Recent Findings in Pathophysiology, Diagnostic and Therapeutic Modalities*, ed. T. Govindaraju, the Royal Society of Chemistry, 2021, p. in press.
6 C. Cheignon, M. Jones, E. Atrian-Blasco, I. Kieffer, P. Faller, F. Collin and C. Hureau, *Chem. Sci.*, 2017, **8**, 5107.
7 L. S. Van Rompuy and T. N. Parac-Vogt, *Curr. Opin. Biotechnol.*, 2019, **58**, 92.
8 A. Bijelic, M. Aureliano and A. Rompel, *Angew. Chem. Int. Ed.*, 2019, **58**, 2980.
9 N. I. Gumerova and A. Rompel, *Inorg. Chem.*, 2021, **60**, 6109.
10 M. Arefian, M. Mirzaei, H. Eshtiagh-Hosseini and A. Frontera, *Dalton Trans.*, 2017, **46**, 6812.
11 P. Gao, Y. Wu and L. Wu, *Soft Matter*, 2016, **12**, 8464.
12 D. J. Levine, J. Stöhr, L. E. Falese, J. Ollesch, H. Wille, S. B. Prusiner and J. R. Long, *ACS Chem. Biol.*, 2015, **10**, 1269.
13 A. Bijelic and A. Rompel, *Coord. Chem. Rev.*, 2015, **299**, 22.
14 Y. Zhou, L. Zheng, F. Han, G. Zhang, Y. Ma, J. Yao, B. Keita, P. de Oliveira and L. Nadjo, *Colloids Surf. A Physicochem. Eng. Asp.*, 2011, **375**, 97.
15 J. Geng, M. Li, J. Ren, E. Wang and X. Qu, *Angew. Chem. Int. Ed.*, 2011, **50**, 4184.
16 Q. Chen, L. Yang, C. Zheng, W. Zheng, J. Zhang, Y. Zhou and J. Liu, *Nanoscale*, 2014, **6**, 6886.
17 N. Gao, H. Sun, K. Dong, J. Ren, T. Duan, C. Xu and X. Qu, *Nat. Commun.*, 2014, **5**, 3422.
18 G. Hervé, A. Tézé and R. Contant, in *Polyoxometalate Molecular Science*, eds. J. J. Borrás-Almenar, E. Coronado, A. Müller and M. Pope, Springer Netherlands, Dordrecht, 2003, pp. 33.
19 N. I. Gumerova and A. Rompel, *Chem. Soc. Rev.*, 2020, **49**, 7568.
20 G. Scholz, R. Lück, R. Stößer, H.-J. Lunk and F. Ritschl, *Faraday trans.*, 1991, **87**, 717.
21 J. A. Gamelas, I. C. M. S. Santos, C. Freire, B. de Castro and A. M. V. Cavaleiro, *Polyhedron*, 1999, **18**, 1163.
22 B. Alies, I. Sasaki, O. Proux, S. Sayen, E. Guillon, P. Faller and C. Hureau, *Chem. Commun.*, 2013, **49**, 1214.
23 M. G. M. Weibull, S. Simonsen, C. R. Oksbjerg, M. K. Tiwari and L. Hemmingsen, *J. Biol. Inorg. Chem.*, 2019, **24**, 1197.
24 M. Törnquist, T. C. T. Michaels, K. Sanagavarapu, X. Yang, G. Meisl, S. I. A. Cohen, T. P. J. Knowles and S. Linse, *Chem. Commun.*, 2018, **54**, 8667.
25 G. Meisl, J. B. Kirkegaard, P. Arosio, T. C. T. Michaels, M. Vendruscolo, C. M. Dobson, S. Linse and T. P. J. Knowles, *Nat. Protoc.*, 2016, **11**, 252.
26 M. Rana and A. K. Sharma, *Metallomics*, 2019, **11**, 64.
27 S. Noël, S. Cadet, E. Gras and C. Hureau, *Chem. Soc. Rev.*, 2013, **42**, 7747.
28 P. Faller and C. Hureau, *Front.Chem.*, 2021, **8**, 1236.
29 C. M. Cremers, D. Knoefler, S. Gates, N. Martin, J.-U. Dahl, J. Lempart, L. Xie, M. R. Chapman, V. Galvan, D. R. Southworth and U. Jakob, *Mol. Cell*, 2016, **63**, 768.
30 S. J. C. Lee, E. Nam, H. J. Lee, M. G. Savelieff and M. H. Lim, *Chem. Soc. Rev.*, 2017, **46**, 310.
31 C. Esmieu, D. Guettas, A. Conte-Daban, L. Sabater, P. Faller and C. Hureau, *Inorg. Chem.*, 2019, **58**, 13509.